Atmos. Chem. Phys. Discuss., 13, 20011–20048, 2013
www.atmos-chem-phys-discuss.net/13/20011/2013/
doi:10.5194/acpd-13-20011-2013
© Author(s) 2013. CC Attribution 3.0 License.

Atmospheric Chemistry and Physics Discussions

This discussion paper is/has been under review for the journal Atmospheric Chemistry and Physics (ACP). Please refer to the corresponding final paper in ACP if available.

Seasonal variability and long-term evolution of tropospheric composition in the tropics and Southern Hemisphere

K. M. Wai[1] **and S. Wu**[2]

[1]Department of Geological and Mining Engineering and Sciences, Michigan Technological University, Houghton, MI, USA
[2]Atmospheric Sciences Program, Department of Geological and Mining Engineering and Sciences and Department of Civil and Environmental Engineering, Michigan Technological University, Houghton, MI, USA

Received: 17 June 2013 – Accepted: 19 July 2013 – Published: 31 July 2013

Correspondence to: K. M. Wai (kwai@mtu.edu)

Published by Copernicus Publications on behalf of the European Geosciences Union.

Abstract

Present-day and future impacts of biomass burning and other sources in the tropics and Southern Hemisphere are studied by global chemical transport model (GCTM), satellites retrievals and surface measurements. The spring CO peaks found at Mahe Island (Western Indian Ocean) are attributed to the burnings in India but not those from Northern Africa. Easter Island (Eastern Pacific Ocean) is impacted indirectly by the hemispheric zonal transport of CO due to the burnings in Southern Africa/Latin America, via the westerlies. An increasing trend for CO by 0.33 ppb yr^{-1} in the past decade at Ascension Island is attributed to the combined effects of Latin American/Southern Africa burnings and increase of CH_4 level. Changes in water vapour and UV over Southern Atlantic Ocean (SAO) in future January have dominated effects on the O_3 distribution. More than 55 % of O_3 concentrations over SAO in both present-day and future September are not directly affected by the emissions (including lightning) over the adjacent two continents but attributable to transport of O_3 from outside due to CO and CH_4 oxidation and stratospheric intrusion. High NO_x emissions in both continents in future increase the PAN concentrations over remote oceans at higher southern latitudes (> 35° S) as far as those near Australia, affecting the O_3 budget over there. Future changes of biomass burning and anthropogenic NO_x emissions in Southern Africa lead to a new area of O_3 maximum near South Africa. The resulted O_3 outflow to the Indian Ocean is pronounced due to the effects of the persistent anti-cyclone. A general reduction of future OH radical concentrations is predicted over the remote marine boundary layer in the tropics and Southern Hemisphere, due to the increases in CH_4 and CO emissions combined with the low-NO_x environment.

1 Introduction

Emission from biomass burning is an important source for a number of atmospheric trace gases including carbon monoxide (CO), nitrogen oxides (NO_x), ozone (O_3), and

ACPD
13, 20011–20048, 2013

aerosols including black carbon. Biomass burning accounts for about 30 % of the global total CO sources (Galanter et al., 2000). These trace gases and aerosols play important roles in tropospheric chemistry, air quality and global climate (Levine et al., 1995; Granier et al., 2000; Haywood et al., 2008). They can affect the abundance of hydroxyl radical (OH), which is the major oxidizing agent in the troposphere.

There is much less emission from fossil fuel combustion in the Southern Hemisphere (SH) and equatorial regions than the northern mid-latitudes. As a consequence, the tropospheric composition in the SH equatorial regions are particularly sensitive to biomass burning emissions. On the other hand, there are more biomass burnings in Africa than any other continent (Hao and Liu, 1994). Previous studies, in particular the campaign of Transport and Atmospheric Chemistry in the Atlantic (TRACE-A) (Fishman et al., 1996), and the Southern African Fire Atmosphere Research Initiative in 1992 (SAFARI-92) (Andreae et al., 1996), have examined the contribution of biomass burning activities from Southern Africa and Latin America to the tropospheric composition and ozone anomaly over the SAO.

The application of remote sensing products in investigating the distribution and evolution of atmospheric chemical species has the apparent advantage in spatial coverage, especially for remote areas. The Total Ozone Mapping Spectrometer (TOMS) (Hsu et al., 1996; Thompson et al., 2001), MOPITT (Edwards et al., 2006) and Tropospheric Emission Spectrometer (TES) (Jourdain et al., 2007) deployed to the satellites were used to detect biomass burning signatures. While most of the previous studies focused on short time periods of less than a year, inter-annual variability of biomass burning emissions and atmospheric transport was reported for the tropical regions (Allen et al., 1996; Barbosa et al., 1999; van der Werf et al., 2006). Better understanding of the impacts on tropospheric composition due to inter-annual variability in biomass burning emissions is needed.

Recently there has been increasing interest to the potential impacts of global change on atmospheric composition and air quality. All future global socioeconomic scenarios by the Intergovernmental Panel on Climate Change (IPCC) project a global increase of

ACPD
13, 20011–20048, 2013

emissions, including biomass burning emissions, of ozone precursors (NO_x, NMVOC and CO) over the 21st century (Nakicenovic and Stewart, 2000). The 2050 climate change alone was estimated to increase the global lightning NO_x emission by 18 % (Wu et al., 2008a). Since tropical ozone is very sensitive to NO_x emissions from lightning (Moxim and Levy, 2000; Jenkins et al., 2003; Wu et al., 2007), the climate change implication on the tropical composition could be significant. Most of the previous studies on the impacts of global change on tropospheric composition have focused on the northern mid-latitudes, in particular the developed regions (e.g., Liao et al., 2006; Unger et al., 2006; Hedegaard et al., 2008; Wu et al., 2008a, b) but not the SH.

The aims of this study are to (a) improve our understanding on the impacts of biomass burning on tropospheric CO concentration in the tropics and SH and its seasonal variability and long-term trend by combining in-situ measurement data, satellite observations and model simulations, and (b) examine the potential impacts of global change on CO, NO_x, O_3 and OH focusing on the tropics and SH.

2 Approach and method

We first analyze and compile the surface CO measurements in the tropics and SH for 2002–2006. A ten-year (2001–2010) dataset of surface CO measurement is used to determine if there is a statistically significant trend. To evaluate the performance of a GCTM, surface measurements and satellite observations are used. Unless specified otherwise, the analyses of atmospheric composition focus on January and September when biomass burning activities peak in Africa and Latin America (e.g. Moxim and Levy II, 2000; Sudo et al., 2002; Duncan et al., 2003; Edwards, et al., 2003; Korontzi et al., 2004; Bian et al., 2007). The GCTM is then used to simulate the perturbations to tropospheric composition associated with the projected changes in emissions and climate in the 2050s.

ACPD
13, 20011–20048, 2013

2.1 Observational data

The NOAA/ESRL Global Monitoring Division (GMD) network surface CO data (Novelli et al., 2003; Bian et al., 2007; Novelli and Masarie, 2012) at Ascension Island (7.98° S, 14.42° W), Mahe Island (4.67° S, 55.17° E) and Easter Island (27.13° S, 109.45° W) respectively (Fig. 1) is used. The CO retrievals obtained from the Measurements Of Pollution In The Troposphere (MOPITT) CO with version 4 L3 monthly daytime retrieved products (1° × 1° gridded) (Edwards et al., 2003, 2006; Bian et al., 2007) is also used. Detailed description of the products was discussed in the mentioned references and are not repeated here.

2.2 Description of model

The GEOS-Chem model (http://acmg.seas.harvard.edu/geos/) v9-01-01 is used for simulations of the atmospheric chemistry and composition to study the impacts of biomass burning and other sources for present-day and future scenarios. GEOS-Chem has detailed and fully coupled ozone-NO_x-VOC-aerosol chemistry which can resolve more than 100 species. It has been extensively evaluated with in-situ ground/airborne and satellite observations (e.g., Bey et al., 2001; Jaeglé et al., 2003; Fiore et al., 2003; Li et al., 2004; Heald et al., 2006).

The model is driven by either assimilated (GEOS-4 data from NASA GMAO with 2° × 2.5° horizontal resolution and 30 vertical layers) or simulated (NASA/GISS GCM simulation with 4° × 5° horizontal resolution and 23 vertical layers) meteorological fields. All the model runs are conducted following one year of model spin-up. The interface between GEOS-Chem and the GISS GCM has been described and evaluated by Wu et al. (2007) and also applied in a number of previous studies to investigate the potential effects of global change on air quality (Wu et al., 2008a, b; Pye et al., 2009). Five years (2002–2006) of GEOS-Chem simulation is conducted with the GEOS-4 meteorological data for the present-day scenario.

ACPD
13, 20011–20048, 2013

For the present-day simulations with GEOS-4 data, emissions from fossil fuel combustion follow the EDGAR global anthropogenic emissions inventory and are updated with regional emission inventories where applicable (e.g. CAC inventory for Canada; BRAVO inventory for Mexico; STREETS inventory for Asia; NEI2005 inventory for the United States and EMEP inventory for Europe). Biomass burning emissions of CO, NO_x and NMVOCs are based on the Global Fire Emission Database version 2 (GFEDv2) (Van der Werf et al., 2006). Biofuel emissions are from Yevich and Logan (2003). Biogenic emissions follow the Model of Emissions of Gases and Aerosols from Nature (MEGAN) scheme (Guenther et al., 2006). Lightning NO_x emissions in GEOS-Chem are parameterized as a function of deep convective cloud top height (Price and Rind, 1992; Wang et al., 1998) and distributed vertically following Pickering et al. (1998) with recent updates by Murray et al. (2011).

To examine the potential impacts of global change on atmospheric composition in the SH and the equatorial region, we carry out GEOS-Chem simulations for the present-day (2002–2004) and future (2049–2051) scenarios respectively. Meteorological fields archived from the GISS GCM simulation results are used to driven the GEOS-Chem model. Following Wu et al. (2008a), we apply the IPCC A1B scenario for the 2000–2050 changes in anthropogenic emissions of ozone and aerosol precursors. Natural emissions of ozone precursors including NO_x from lightning and soil, and NMVOCs from vegetation, are computed locally within the model on the basis of meteorological variables and hence allowed to change in response to climate change. The potential effects of climate change on biomass burning (e.g., Westerling et al., 2006; Spracklen et al., 2009) are not considered in this study. A comparison of the present-day and future emissions in areas of interest is shown in Table 1. Possible 2000–2050 changes in stratosphere-troposphere exchange (STE) of ozone is not accounted for in this study. In all simulations, STE for ozone is represented by the Synoz flux boundary condition (McLinden et al., 2000) with an imposed global annual mean STE flux of 500 $Tg\,O_3\,yr^{-1}$.

ACPD
13, 20011–20048, 2013

3 Results and discussion

3.1 Impacts of biomass burning on CO for the present-day

With a relative long life-time (about a week to 2 months), CO is a good tracer for long-range transport in the troposphere. Both observational data and model simulations show large and regular seasonal variations of CO concentrations at the remote surface stations on the Ascension Island, Mahe Island and Easter Island (Fig. 1). The seasonal variations in CO at the three stations are well-captured by the GEOS-Chem model, especially for those in Mahe Island and Easter Island. There is systemic over-estimates in Ascension Island, similar to the work by Sinha et al. (2004).

3.1.1 Northern Africa burnings

In Northern Africa, the savanna burning is usually between south of Sahara Desert and north of the tropical rain forest near the equator during winter-spring time of Northern Hemisphere (NH). It is evident by numerous fire events shown in the MODIS fire map (Fig. 2) and elevated CO by MOPITT observed within the period. The CO plumes from Northern African burnings are transported westward or south-westward by the Harmattan flow and are lifted above the planetary boundary layer (PBL) when the plumes encounter the cool monsoon air from the Gulf of Guinea, as well as the Inter-tropical Convergence Zone (ITCZ). We use the NOAA HYSPLIT model (Draxler and Rolph, 2013; Rolph, 2013) for forward trajectory analysis which clearly shows the rapid vertical transports from 500 m to > 3000 m a.s.l. within 3.5 days (Fig. 2). Once at the lower free troposphere, the Africa Easterly Jet effectively enhances the long-range transport (LRT) of the CO plumes to Latin America. These are indicated by the trajectories started from Western Africa. The southward shift between the peak burning activities at ground level and the area of large-scale elevation of CO concentrations at 700 hPa, as well as the LRT of CO over Atlantic Ocean, are clearly observed by the satellite retrievals (figure not shown) and also simulated by the model (Fig. 2).

ACPD
13, 20011–20048, 2013

Based on the above discussion, the impacts of burnings in Northern Africa on the CO variations of Mahe Island (Fig. 1) are expected to be minimal. However, Fig. 1 clearly shows the spring peaks of CO at Mahe Island. The back-trajectory calculation (figure not shown) indicates that air masses at Mahe Island frequently (> 70 %) originate from India in January and February, while the rest of them were mainly from Europe via Middle East, Sahara Desert and Indian Ocean. The burning emissions in India are intensive in January to March, as shown by the GFEDv2 emissions and findings of Galanter et al. (2000). The spring peaks in measured CO at Mahe Island are thus attributed to the burning activities from India.

With the rapid vertical transport of the CO plumes from the source areas over the equatorial Atlantic Ocean (30° W–0°), the above discussion also explains no burning signature due to the Northern Africa burning activities to be detected at Ascension Island in the SAO since the elevated CO concentration is confined to above the PBL. During the periods, the CO concentration measured at Ascension Island (e.g. ~ 60 ppb in January 2005) was lower than that observed at 700 hPa by MOPITT (~ 100 ppb in the same time) at the same location.

3.1.2 Southern Africa burnings

In Southern Africa, the wide-spread burning events occur mainly in Angola, Zambia and Democratic Republic of the Congo during July to September. Persistent low-level easterlies/south-easterlies facilitate the westward transport of CO plumes from Southern Africa. Three synoptic-scale high pressure systems are located persistently over Southern Africa, Latin America/adjacent Atlantic Ocean and Indian Ocean. They are featured with descending air and relatively low wind speeds which limit the dispersion of the burning pollutants. Under its influence over Southern Africa, the CO plumes tend to recirculate over the continent. This is well indicated by our forward trajectory calculations (figure not shown) in the same period from 2002 to 2006. The trajectories further suggest two main exit pathways of the CO plumes that one is from southern tip of the continent to Indian Ocean and another is from western part of the continent to Atlantic

ACPD
13, 20011–20048, 2013

Ocean just south of the ITCZ. The exit pathways are well indicated by the GEOS-Chem model (Fig. 3).

Regional elevations of CO over the SAO at surface level during these months in 2002–2006 due to the westward transport of the burning plumes are also evident by the measurements in Ascension Island (Fig. 1) and the modeling results (Fig. 3). The modeling results at the Island capture the peaks though over-predictions are noted as mentioned. It is interesting that elevated CO concentration were still measured in October when the burning activities in Southern Africa were decreased rapidly. It is attributed to recirculation (Swap et al., 1996; Edwards et al., 2006) of CO over the Atlantic Ocean due to the historical accumulation of CO in previous months. Backward trajectory plots in October launched at Ascension Island also indicate the re-circulation of air masses over the SAO (Fig. 3). Since CO plumes followed the exit pathway from the southern tip of the continent to Indian Ocean are transverse at higher southern latitudes (e.g. 10° S–20° S), no elevated CO were measured at Mahe Island.

3.1.3 Latin America burnings

The fire maps shown most of the burning activities in Latin America were undertaken at Brazil, Bolivia, Paraguay and Argentina and intensified in August to October in 2002–2006 and were resulted in the so-called "smoke corridor" over these countries. Based on the MOPITT CO observations at 700 hPa (figure not shown) and GEOS-Chem CO predictions at similar altitude (Fig. 3), continental outflows of CO occur at southeast and northwest of Latin America. Rapid vertical export by deep convective processes is a major process to transport burning-produced pollutants from PBL to upper troposphere in Latin America (Anderson et al., 1996; Freitas et al., 2005; Wu et al., 2011). Deep convection is indicated by lightning (Del Genio et al., 2007) and its rates are detected by Lighting Imaging Sensor (LIS). The satellite retrievals indicate that deep convection occurred more frequent in September (Fig. 4) compared to August within the 5 yr period. For instance, the transport of CO reaches about 10 km a.s.l. with modeled CO concentrations up to 180 ppb during September 2006. Once the plumes are vented

ACPD
13, 20011–20048, 2013

to the free troposphere, the westerlies at upper troposphere (> 8 km a.s.l.) transport the plumes from Latin America towards Southern Africa (Fig. 4).

The modeling results show that the north-westward transport of burning plumes from Latin America to Pacific Ocean was rarely found at higher southern latitudes (> 10° S) within the 5 yr period. Therefore, the Easter Island which locates sub-tropically (~ 27° S) to the west of Latin America is not directly impacted by the plumes. Since no other major CO source locates nearby, it is expected inter-seasonal variations of CO at Easter Island are minimal. Interestingly, CO concentrations peaked in September/October of 2002, 2005 and 2006 (no data available from May 2003–May 2005, Fig. 1) and the model also predicts the inter-seasonal variations. It is attributed to the persistent westerlies about 30° S or further southward pick up the CO-laden air masses from Africa and Latin America burnings. The air masses are firstly transported over the Indian Ocean and then reached Australia aloft, advent over the Pacific Ocean and eventually reached the Easter Island. Previous study (Edwards et al., 2006) found that a band of high CO concentrations developed which circumscribed the globe around during Austral spring and elevated CO levels from background were observed in Australia and New Zealand. The elevated CO background is attributed to be originated from Southern Africa/Latin America (Rinsland et al., 2001). Our backward trajectories launched from Easter Island reach Australia/New Zealand aloft during these periods (figure not shown), which support the CO transport pathway by the westerlies.

3.2 Trend of CO at Ascension Island in the past decade

Based on the above finding, Ascension Island is the only site which is impacted directly by the biomass burning emissions from Southern Africa and Latin America. Surface CO measurements from this site with longer sampling period (2001–2010) are therefore studied to determine if there has been any statistically significant trend. Figure 5 shows the 10 yr time evolution of CO concentrations (ppb) at Ascension Island. The seasonal variation is evident, similar to Fig. 1, with small inter-annual variability. To investigate whether there is a trend, a regression analysis was performed to fit the observation

ACPD
13, 20011–20048, 2013

with a polynomial equation in the form as shown below:

$$C_t = a_0 + a_1 t + a_2(2\pi t/365) + a_3 \cos(2\pi t/365) + e_t \quad (1)$$

where:
C_t: CO concentration at a time t (in days)
a_0, a_1, a_2, a_3: regression coefficients
e_t: residual from the model

The sinusoidal terms in Eq. (1) are used to account for the seasonal variations of CO concentration. A linear term is use to indicate any possible trends over this time period. The coefficients of the equation are determined by the least-square method. The observational data was smoothed by 5 day centered moving average prior to the regression analysis. A statistically significant ($p < 0.01$) increasing trend is identified with the increase rate of 0.33 ± 0.24 ppb yr^{-1} and the r^2 of 0.61.

The increasing trend of CO at Ascension Island appears to be driven by the increases in biomass burnings from Latin America/Southern Africa and increase of ambient CH_4 in recent years. An inverse modeling study with observational constraint on CO emissions from MOPITT retrievals during 2000–2009 suggested a significant increase of CO emissions since 2000 from 137 Tg yr^{-1} (in 2000) to 198 Tg yr^{-1} (in 2007) in Latin America, although the emissions was lower at about 130 Tg yr^{-1} in 2008 and 2009. The emissions in Southern Africa showed slight increase from 132 Tg yr^{-1} (2000) to 146 Tg yr^{-1} (2009) (Fortems-Cheiney et al., 2011). According to the long-term trend (1980's–2005) of aerosol optical depth (AOD) from the AVHRR satellite instrument, a positive trend up to 0.03 per decade in the fall seasons were reported over Southern Africa (lat: 15.0 to 5.0° S; lon: 5.0 to 15.0° E) most affected by biomass burning (Zhao et al., 2008). A slightly positive trend during austral spring when the burning smoke transported from the Amazon regions was also found over Latin America (lat: 20.0 to 10.0° S; lon: 40.0 to 30.0° W) (Zhao et al., 2008). The AOD measurements from MODIS in 2001–2007 also reported an increasing trend of 0.0012 yr^{-1} within 30° S–equator lat-

ACPD
13, 20011–20048, 2013

itudes (Yu et al., 2009), where biomass burning in Latin America/Southern Africa is the major source of aerosols in these regions.

Long-term variations of CO can also be affected by the variations of atmospheric CH_4, which provides an important source for CO. Large increases in atmospheric CH_4 concentrations have been reported since 2007 after staying relatively stable in earlier years of the past decade. The CH_4 increase of $\sim 7.5\,ppb\,yr^{-1}$ was observed from the satellite instrument SCIAMACHY over the tropics (Schneising et al., 2011). The measurements from the AGAGE and CSIRO networks show renewed growth both in the SH and NH (Rigby et al., 2008). Globally averaged CH_4 increase was also found in the NOAA's global sampling network during 2007 (by $8.3\,ppb\,yr^{-1}$) and 2008 (by $4.4\,ppb\,yr^{-1}$). The increase was found to be more in the SH (the tropics) in 2007 (2008) compared with other zonally averaged regions (Dlugokencky et al., 2009).

3.3 Impacts of global change on tropospheric composition in the tropics and Southern Hemisphere

We examine in this study the potential effects of 2000–2050 changes in both climate and emissions on tropospheric composition in the tropics and SH. We follow the IPCC A1B scenario (Nakicenovic and Stewart, 2000) for the 2000–2050 changes in climate and emissions of ozone precursors (Wu et al., 2008a).

3.3.1 Perturbations to tropospheric composition in January due to changes in emissions and climate

In future January, more intense CO plumes from Northern Africa just north of the equator follow the easterlies and is transported towards Latin America over the Atlantic Ocean (Fig. 6), due mainly to the burnings (Table 1). They result in an increase of the lower tropospheric CO concentrations up to 80 ppb related to the present-day case. General increases are also found for NO_x concentrations in the lower troposphere (≤ 2.1 km a.s.l.) driven by increases in both biomass burnings and fossil fuel emis-

ACPD
13, 20011–20048, 2013

sions (Table 1). Increase of O_3 by 20–35 % across the Atlantic Ocean just north of the equator is predicted.

The future trends of the middle and upper tropospheric O_3 distribution over the SAO in January, which is related to the well-known Tropical Atlantic Ozone Paradox (Thompson et al., 2000), is further studied. Lightning is a major source of NO_x in the mid- and upper troposphere. The simulated 2050 ozone in the mid- (2.1–7.6 km a.s.l.) and upper (7.6–14.4 km a.s.l.) troposphere show little contribution from biomass burning emissions. It is noted that the projection of increased NO_x emissions from lightning over Southern Africa and Latin America by 18.2 % and 16.4 %, respectively (Table 1) might not cause a general increase of O_3 levels of the whole SAO in these levels. The future O_3 concentrations are predicted to be increased by 10–20 % in the upper troposphere over the SAO at latitudes 5–25° S (Fig. 6). However, the O_3 concentrations in the mid-troposphere, where O_3 concentrations were reported as one out of the two maxima in austral spring (Edwards et al., 2003), will have been no change or even be decreased in lower latitudes (< 15° S) but increased in higher latitudes (> 20° S) in future (Fig. 6). The interesting picture is attributed by the combined effects of future change of UV (indicated by column cloud fraction) and water vapor content, and complicated spatial future change of lightning flash rates. Here, the effect of changes of column cloud fraction and water vapor is further discussed. Change of column cloud fraction up to +45 % (−30 %) is found within the region 10–20° S (> 20° S) over the SAO (Fig. 6) in future, suggesting decrease (increase) of UV radiation which reduce (enhance) the O_3 production over there. The anti-correlation between change of O_3 and water vapor (Fig. 6 middle and bottom right panels) within the area is due to O_3 photolysis with water vapor to produce hydroxyl radicals with the presence of UV radiation. For example, the increase of water vapor at 10° S facilities O_3 photolysis and reduces the O_3 concentrations there.

ACPD
13, 20011–20048, 2013

3.3.2 Perturbations to tropospheric composition in September due to changes in emissions and climate

In Southern Africa, the reduced emissions (Table 1) might not well reflect in the ambient CO concentrations because of the large growth of CO emissions due to fossil fuel in South Africa, Republic of the Congo and Gabon, such that only 15 % reduction within 10–20° S in Southern Africa is resulted. In Latin America, however, the large growth of CO emissions due to the burnings results in more than 450 ppb in lower troposphere over almost the entire tropical and sub-tropical (20° S–0°). Lower tropospheric CO concentrations near the center of SAO (15° S, 15° W) are predicted to be increased more than 80 % to 120 ppb. Reflected by increased lightning frequency, elevated CO concentrations (300 ppb) found at upper troposphere (figure not shown) over Latin America in future demonstrates the importance of deep convection to export biomass burning emissions in Latin America from the boundary layer to mid- and upper troposphere. The CO is then input into the SAO by upper-level westerlies, resulting in maximum 80–90 % increases of CO there.

Significant reduction of burning emissions (by 46 %) in Southern Africa is counterbalanced by projected large increases (by 3.8 times in Table 1) in fossil fuel emissions. The consequential effects on lower tropospheric NO_x concentrations are shown in Fig. 7. The maximum NO_x concentrations located about 10–20° S, due to biomass burnings, in present-day are predicted to be replaced by two maxima in future – one in similar areas with reduced magnitudes due to biomass burnings and another in South Africa due to large increases in fossil fuel emissions. Similar patterns are found for O_3 (Fig. 7) which reflects the critical role of NO_x in controlling O_3 in the tropics. One of the outflow pathways of O_3 from Southern Africa into the mentioned SAO area is clearly seen and supports the major lower tropospheric contribution of O_3 over the SAO from the continent. Another O_3 output pathway to the Indian Ocean, which is not pronounced in the present-day but in the future, is due to the significant increase of fossil fuel NO_x emissions in South Africa and effects of the persistent anti-cyclone (Fig. 7). The contri-

ACPD
13, 20011–20048, 2013

bution of fossil fuel emissions is ~ 10 % of total O_3 to the east of the continent (< 60° E) over the Indian Ocean in future.

PAN is produced by photochemical oxidation of NMVOC in the presence of NO_x and thus its concentrations are higher near the NO_x sources (Fig. 8). For the present-day, PAN concentrations in the lower troposphere are found to be low (< 0.03 ppb) over the SAO and Indian Ocean. In the 2050s, PAN concentrations in the lower troposphere are enhanced by higher NO_x emissions from both continents and reach 0.07 ppb over remote oceans at higher latitudes (> 35° S) far away from the continents to the region near Australia, although it was reported that higher temperature in future would reduce the potential of LRT of PAN (Wu et al., 2008a). The major contribution from fossil fuel emissions is demonstrated by a sensitivity model run which excludes fossil fuel emissions (Fig. 8). The higher PAN concentrations are due to south-eastern outflows of PAN from Southern Africa to Indian Ocean, produced by high NO_x emissions in South Africa and nearby areas, the effects of anti-cyclone and the contribution of PAN production from Latin America. The distinct zonal gradient of PAN concentrations over Indian Ocean and further east at higher latitudes are maintained by the westerlies and lower temperatures which stabilize the PAN. It has implications for the O_3 budget over the remote oceans since PAN acts as a low-temperature reservoir of NO_x. PAN serves as a source of NO_x once it undergoes thermal dissociation at higher temperature and thus contributes to O_3 formation. The contribution of fossil fuel emissions from Latin America to mid- and upper troposphere PAN for 2050s is found to be relatively small compared with that from biomass burning.

It is interesting to discuss further O_3 contribution over the SAO where it attracts continuous attention to the scientific community (Singh et al., 1996; Jacob et al., 1996; Jourdain et al., 2007) due to the unique meteorological and emission settings. The vertical profiles of total O_3 concentrations over the remote SAO with their major contributions from the burning and lightning sources mentioned in future are shown (Fig. 9). The contribution of a process (i.e. biomass burning, lightning, fossil fuel and soil) is obtained by subtracting without-such-process from the total in order to minimize the non-linear

ACPD
13, 20011–20048, 2013

effects. The highest O_3 concentrations are in upper troposphere where its longer lifetime and net O_3 production by lightning NO_x emissions there. It is predicted a general increase of O_3 concentrations throughout the tropospheric column over the SAO in future. The increases are relatively small (~ 5 ppb) below 3 km a.s.l. but large (~ 20 ppb) above 8 km a.s.l. In both time frames, relatively higher contributions of O_3 from biomass burning and lightning are in the lower and upper troposphere, respectively. Without the lightning source, O_3 concentrations in the mid- and upper troposphere are reduced up to 19 ppb in future. The contribution of soil emissions is negligibly small due to minimal NO_x contribution. A striking feature from the result is that > 55 % of O_3 concentration at each tropospheric level in both time frames is not directly affected by the emissions (including lightning) from Southern Africa and Latin America. The result is comparable to the background contributions at upper (57 %), mid- (77 %) and lower (67 %) troposphere over the SAO calculated by a 3-D global CTM (Moxim and Levy II, 2000). The contributions outside the two continents are likely due to transport of O_3 from the background CO and CH_4 oxidation, as well as the contribution from stratospheric intrusion.

3.3.3 Hydroxyl radical – the present-day and future status

Present-day OH, a key player of tropospheric oxidizing capacity, with its concentration computed by our model is of an order of 10^6 cm^{-3}. The value is comparable with the modeled values reported by other studies (e.g. Dentener et al., 2003; Wu et al., 2008a and references mentioned below), although comparisons of mean OH concentration is somewhat hampered by differences in averaging methods (Lawrence et al., 2001). A common feature of the zonal annual averaged OH concentrations computed by our model and reported elsewhere (Wang and Jacob, 1998; Spivakovsky et al., 2000) is the highest OH concentration near the tropics due to the highest UV and high water vapor found there. The concentrations are then decreased with latitudes in both hemispheres.

In present-day January, the source of biomass burnings in Northern Africa just north of the equator does not show any elevated OH concentration (figure not shown) in lower troposphere since OH production from high NO_x and O_3 and is offset by loss of OH due

ACPD
13, 20011–20048, 2013

to high CO. In future January, the mentioned increase of CO, NO_x and O_3 concentrations in lower troposphere, mainly due to the increase of the burning emissions, leads to a relatively small changes (< 10 %) of OH concentrations over the burning areas in Northern Africa and the adjacent Atlantic Ocean to the west of the continent. Over the SAO despite the increase of O_3 concentrations predicted in mid-troposphere in future, it will be a general decrease of OH concentrations by up to 20 %. The lower tropospheric OH concentrations over the SAO is decreased by similar magnitudes, which is attributed by the increase of CH_4 assumed in the model from ~ 1750 (present-day) to 2400 ppb (future) (Wu et al., 2008a). The results in mid-troposphere with less water vapor (and thus less OH generated) are therefore reasonable.

In future September, the remote oceanic areas including the SAO, Indian Ocean to the east of Southern Africa and Pacific Ocean to the west of Latin America will be featured with hemispheric decrease of OH concentrations at the boundary layer by up to 30 % compared to the present-day situation (Fig. 10). It is due to the lack of OH sources (contrary to the anthropogenic NO_x sources in the NH) to offset the OH loss from increase of assumed CH_4 and calculated CO in future. These two species have long atmospheric lifetimes and thus the influence on OH is widespread. While in the continent of Southern Africa, the combined effects of change of emissions of CO, NO_x and NMVOCs and geographical shift of land use, as well as the change in ambient CH_4 concentration, result in a larger reduction (~ 30 %) of lower tropospheric OH concentrations there in future. On the contrary, relatively smaller negative changes are found in Latin America with even some positive changes of 50 % in the northwest of the continent. In mid- and upper troposphere, future OH reduction is found over the remote ocean, similar to the January situation. However, there are areas of positive OH change over the Latin America, which are corresponded to the areas of the significant increase of NO_x concentrations (Fig. 10), suggesting the important role of NO_x in OH production there.

Negative change of annual OH concentrations in future at remote marine boundary layer at tropics and the SH resulted in our model is also predicted by a 3-D global CTM

ACPD
13, 20011–20048, 2013

study (Wild and Palmer, 2008) and an 1-D photochemical model (Thompson et al., 1990). Meanwhile, our model predicts similar OH concentrations at upper troposphere over the SH for present-day and future (figure not shown). The increase of OH production at upper troposphere in future by lightning emitted NO is attributed to play an important role to offset the OH loss. It is supported by the global increase of OH by 12 % in the upper troposphere due to increase of lightning frequency in 2050 (Wu et al., 2008a).

4 Conclusions

A combination of in-situ measurements, satellite observations, global chemical transport modeling and back trajectory results were used to examine recent CO variability in the tropics and SH due to the impacts of biomass burning. Our modeling results generally show reasonable agreement with observations. Clear seasonal variations in CO were found at all the three remote islands located in SH near Southern Africa and Latin America but only the Ascension Island is impacted directly by the continental-scale burning activities. Statistically significant increasing trend of CO at Ascension Island is identified for the period of 2001–2010.

Sensitivity model simulations have been conducted to examine the perturbations to tropospheric composition in the tropics and SH due to projected changes in emissions and climate between 2050 and 2000. In 2050s, the lower tropospheric CO concentrations are computed to be more than 500 ppb over Africa in January which is mainly due to the increase in biomass burnings emissions. Combining the increase of different sources emissions, increase of O_3 by 20–35 % across the Atlantic Ocean just north of the equator is predicted. It is noted that the projection of increased NO_x emissions from lightning over Southern Africa and Latin America by 18.2 % and 16.4 %, respectively might not cause a general increase of O_3 levels of the entire SAO in both mid- and upper troposphere. The O_3 concentrations in the mid-troposphere will have no change or even be decreased in lower latitudes ($< 15^{\circ}$ S) but increased in higher lati-

ACPD
13, 20011–20048, 2013

tudes (> 20° S) in future. The interesting picture is attributed by the combined effects of regional changes of water vapor contents and UV (indicated by column cloud fraction) in different latitudes and complicated spatial change of lightning flash rates found over the SAO in future.

In the 2050s, export of the burning emissions from the boundary layer to mid- and upper troposphere over Latin America by deep convection lead to maximum CO concentrations of ~ 300 ppb in September. It is found that emissions (including lightning NO_x sources) from Southern Africa and Latin America contribute to less than 45 % of the total tropospheric ozone over the SAO. For the impacts associated with these emissions, biomass burning is most important for the lower troposphere while lightning is most important for the upper troposphere. In the 2050s, PAN concentrations in the lower troposphere enhanced by the higher NO_x emissions in both continents will reach 0.07 ppb over remote oceans at higher latitudes (> 35° S) far away from the continents to the region near Australia.

The average OH concentrations for the present-day computed by our model are comparable to those reported in the literature. In future January, increase of CO, NO_x and O_3 concentrations in lower troposphere due to the increase of the burning emissions leads to a relatively small changes (< 10 %) of OH concentrations over the burning areas in Northern Africa and the adjacent Atlantic Ocean to the west of the continent. In the 2050s, the remote oceanic areas near equator and the SH including the SAO, Indian Ocean to the east of Southern Africa and Pacific Ocean to the west of Latin America are featured with hemispheric decrease of OH concentrations at the boundary layer. The reduction is pronounced in September with up to 30 % compared to the present-day situation. It is due to the lack of OH sources to offset the OH loss from increase of assumed CH_4 and calculated CO in future. However, increase frequency of lightning in future and the resulting NO_x emissions offset the OH loss in upper troposphere.

Acknowledgements. This publication was made possible by US EPA grant (grant 83518901). Its contents are solely the responsibility of the grantee and do not necessarily represent the

ACPD
13, 20011–20048, 2013

official views of the USEPA. Further, USEPA does not endorse the purchase of any commercial products or services mentioned in the publication. We thank Aditya Kumar at Michigan Tech for help with the statistical analysis. The authors acknowledge the NOAA Air Resources Laboratory (ARL) for the provision of the HYSPLIT model used in this publication. We also acknowledge: (1) Dr. P. C. Novelli and his team for the provision of the CO surface measurements at Ascension Island as a station in the NOAA/ESRL GMD network; (2) the use of Rapid Response imagery from the LANCE system operated by the NASA/GSFC/ESDIS with funding provided by NASA/HQ; (3) the LIS Science Data obtained from the NASA EOSDIS GHRC DAAC, Huntsville, AL.

References

Allen, D. J., Kasibhatla, P., Thompson, A. M., Rood, R. B., Doddridge, B. G., Pickering, K. E., Hudson, R. D., and Lin, S.-J.: Transport-induced interannual variability of carbon monoxide determined using a chemistry and transport model, J. Geophys. Res., 101, 28655–28669, 1996.

Anderson, B. E., Grant, W. B., Gregory, G. L., Browell, E. V., Collins Jr., J. E., Sachse, G. W., Bagwell, D. R., Hudgins, C. H., Blake, D. R., and Blake, N. J.: Aerosols from biomass burning over the tropical South Atlantic region: distributions and impacts, J. Geophys. Res., 101, 24117–24137, 1996.

Andreae, M., Fishman, J., and Lindesay, J.: The Southern Tropical Atlantic Region Experiment (STARE): Transport and Atmospheric Chemistry near the Equator Atlantic (TRACE A) and Southern African Fire Atmosphere Research Initiative (SAFARI): an introduction, J. Geophys. Res., 101, 23519–23520, 1996.

Barbosa, P. M., Stroppiana, D., Gregoire, J.-M., and Pereira, J. M. C.: An assessment of vegetation fire in Africa (1981–1991): burned areas, burned biomass, and atmospheric emissions, Global Biogeochem. Cy., 13, 933–950, 1999.

Bey, I., Jacob, D. J., Yantosca, R. M., Logan, J. A., Field, B. D., Fiore, A. M., Li, Q., Liu, H. Y., Mickley, L. J., and Schultz, M. G.: Global modeling of tropospheric chemistry with assimilated meteorology: model description and evaluation, J. Geophys. Res., 106, 23073–23095, 2001.

ACPD
13, 20011–20048, 2013

Bian, H., Chin, M., Kawa, S. R., Duncan, B., Arellano, A., and Kasibhatla, P.: Sensitivity of global CO simulations to uncertainties in biomass burning sources, J. Geophys. Res., 112, D23308, doi:10.1029/2006JD008376, 2007.

Del Genio, A. D., Yao, M.-S., and Jonas, J.: Will moist convection be stronger in a warmer climate?, Geophys. Res. Lett., 34, L16703, doi:10.1029/2006JD008376, 2007.

Dentener, F., Peters, W., Krol, M., van Weele, M., Bergamaschi, P., and Lelieveld, J.: Interannual variability and trend of CH_4 lifetime as a measure for OH changes in the 1979–1993 time period, J. Geophys. Res., 108, 4442, doi:10.1029/2002JD002916, 2003.

Dlugokencky, E. J., Bruhwiler, L., White, J. W. C., Emmons, L. K., Novelli, P. C., Montzka, S. A., Masarie, K. A., Lang, P. M., Crotwell, A. M., Miller, J. B., Gatti, L. V.: Observational constraints on recent increases in the atmospheric CH_4 burden, Geophys. Res. Lett., 36, L18803, doi:10.1029/2009GL039780, 2009.

Draxler, R. R. and Rolph, G. D.: HYSPLIT (HYbrid Single-Particle Lagrangian Integrated Trajectory) Model access via NOAA ARL READY Website, NOAA Air Resources Laboratory, Silver Spring, MD, available at: http://ready.arl.noaa.gov/HYSPLIT.php, last access: 28 July 2013, 2013.

Duncan, B. N., Martin, R. V., Staudt, A. C., Yevich, R., and Logan, J. A.: Interannual and seasonal variability of biomass burning emissions constrained by satellite observations, J. Geophys. Res., 108, 4100, doi:10.1029/2002JD002378, 2003.

Edwards, D. P., Lamarque, J.-F., Attie*é*, J.-L., Emmons, L. K., Richter, A., Cammas, J.-P., Gille, J. C., Francis, G. L., Deeter, M. N., Warner, J., Ziskin, D. C., Lyjak, L. V., Drummond, J. R., and Burrows, J. P.: Tropospheric ozone over the tropical Atlantic: a satellite perspective, J. Geophys. Res., 108, 4237, doi:10.1029/2002JD002927, 2003.

Edwards, D. P., Emmons, L. K., Gille, J. C., Chu, A.,. Atti*é*, J.-L, Giglio, L., Wood, S. W., Haywood, J., Deeter, M. N., Massie, S. T., Ziskin, D. C., and Drummond, J. R.: Satellite observed pollution from Southern Hemisphere biomass burning, J. Geophys. Res., 111, D14312, doi:10.1029/2005JD006655, 2006.

Fiore, A. M., Jacob, D. J., Liu, H., Yantosca, R. M., Fairlie, T. D., and Li, Q.: Variability in surface ozone background over the United States: implications for air quality policy, J. Geophys. Res., 108, 4787, doi:10.1029/2003JD003855, 2003.

Fishman, J., Hoell Jr., J., Bendura, R., McNeal, R., and Kirchhoff, V.: NASA GTE TRACE A experiment (September–October 1992): overview, J. Geophys. Res., 101, 23865–23879, 1996.

ACPD
13, 20011–20048, 2013

Fortems-Cheiney, A., Chevallier, F., Pison, I., Bousquet, P., Szopa, S., Deeter, M. N., and Clerbaux, C.: Ten years of CO emissions as seen from Measurements of Pollution in the Troposphere (MOPITT), J. Geophys. Res., 116, D05304, doi:10.1029/2010JD014416, 2011.
Freitas, S. R., Longo, K. M., Silva Dias, M. A. F., Silva Dias, P. L., Chatfield, R., Prins, E., Artaxo, P., Grell, G. A., Recuero, F. S.: Monitoring the transport of biomass burning emissions in South America, Environ. Fluid Mech., 5, 135–167, 2005.
Galanter, M., Levy II, H., and Carmichael, G. R.: Impacts of biomass burning on tropospheric CO, NO_x, and O_3, J. Geophys. Res., 105, 6633–6653, 2000.
Granier, C., Müller, J., and Brasseur, G.: The impact of biomass burning on the global budget of ozone and ozone Precursors, Adv. Glob. Change Res., 3, 69–85, 2000.
Guenther, A., Karl, T., Harley, P., Wiedinmyer, C., Palmer, P. I., and Geron, C.: Estimates of global terrestrial isoprene emissions using MEGAN (Model of Emissions of Gases and Aerosols from Nature), Atmos. Chem. Phys., 6, 3181–3210, doi:10.5194/acp-6-3181-2006, 2006.
Hao, W. M. and Liu, M.-H.: Spatial and temporal distribution of tropical biomass burning, Global Biogeochem. Cy., 8, 495–503, 1994.
Haywood, J. M., Pelon, J., Formenti, P., Bharmal, N., Brooks, M., Capes, G., Chazette, P., Chou, C., Christopher, S., Coe, H., Cuesta, J., Derimian, Y., Desboeufs, K., Greed, G., Harrison, M., Heese, B., Highwood, E. J., Johnson, B., Mallet, M., Marticorena, B., Marsham, J., Milton, S., Myhre, G., Osborne, S. R., Parker, D. J., Rajot, J.-L., Schulz, M., Slingo, A., Tanré, D., P. Tulet : Overview of the dust and biomass-burning experiment and African monsoon multidisciplinary analysis special observing period-0, J. Geophys. Res., 113, D00C17, doi:10.1029/2008JD010077, 2008.
Heald, C. L., Jacob, D. J., Turquety, S., Hudman, R. C., Weber, R. J., Sullivan, A. P., Peltier, R. E., Atlas, E. L., de Gouw, J. A., Warneke, C., Holloway, J. S., Neuman, A. J., Flocke, F. M., and Seinfeld J. H.: Concentrations and sources of organic carbon aerosols in the free troposphere over North America, J. Geophys. Res., 111, D23S47, doi:10.1029/2006JD007705, 2006.
Hedegaard, G. B., Brandt, J., Christensen, J. H., Frohn, L. M., Geels, C., Hansen, K. M., and Stendel, M.: Impacts of climate change on air pollution levels in the Northern Hemisphere with special focus on Europe and the Arctic, Atmos. Chem. Phys., 8, 3337–3367, doi:10.5194/acp-8-3337-2008, 2008.

ACPD
13, 20011–20048, 2013

Hsu, N. C., Herman, J. R., Bhartia, P. K., Seftor, C. J., Torres, O., Thompson, A. M., Gleason, J. F., Eck, T. F., and Holben, B. N.: Detection of biomass burning smoke from TOMS measurements, Geophys. Res. Lett., 23, 745–748, 1996.

Jaeglé, L., Jaffe, D. A., Price, H. U., Weiss-Penzias, P., Palmer, P. I., Evans, M. J., Jacob, D. J., and Bey, I.: Sources and budgets for CO and O_3 in the Northeastern Pacific during the spring of 2001: results from the PHOBEA-II experiment, J. Geophys. Res., 108, 8802, doi:10.1029/2002JD003121, 2003.

Jenkins, G. S., Ryu, J.-H., Thompson, A. M., and Witte, J. C.: Linking horizontal and vertical transports of biomass fire emissions to the Tropical Atlantic Ozone Paradox during the Northern Hemisphere winter season: 1999, J. Geophys. Res., 108, 4745, doi:10.1029/2004GL020093, 2003.

Jourdain, L., Worden, H. M., Worden, J. R., Bowman, K., Li, Q., Eldering, A., Kulawik, S. S., Osterman, G., Boersma, K. F., Fisher, B., Rinsland, C. P., Beer, R., and Gunson, M.: Tropospheric vertical distribution of tropical Atlantic ozone observed by TES during the Northern African biomass burning season, Geophys. Res. Lett., 34, L04810, doi:10.1029/2006GL028284, 2007.

Jacob, D. J., Heikes, E. G., Fan, S.-M., Logan, J. A., Mauzerall, D. L., Bradshaw, J. D., Singh, H. B., Gregory, G. L., Talbot, R. W., Blake, D. R., and Sachse, G. W.: Origin of ozone and NO_x in the tropical troposphere: a photochemical analysis of aircraft observations over the South Atlantic basin, J. Geophys. Res., 101, 24235–24250, 1996.

Korontzi, S., Roy, D. P., Justice, C. O., and Ward, D. E.: Modeling and sensitivity analysis of fire emissions in Southern Africa during SAFARI 2000, Remote Sens. Environ., 92, 376–396, 2004.

Lawrence, M. G., Jöckel, P., and von Kuhlmann, R.: What does the global mean OH concentration tell us?, Atmos. Chem. Phys., 1, 37–49, doi:10.5194/acp-1-37-2001, 2001.

Levine, J. S., Cofer, W. R., Cahoon, D. R., and Winstead, E. L.: Biomass burning: a driver for global change, Environ. Sci. Technol., 29, 120A–125A, 1995.

Li, Q., Jacob, D. J., Munger, J. W., Yantosca, R. M., and Parrish, D. D.: Export of NO_y from the North American boundary layer: reconciling aircraft observations and global model budgets, J. Geophys. Res., 109, D02109, doi:10.1029/2003JD003912, 2004.

Liao, H., Chen, W.-T., and Seinfeld, J. H.: Role of climate change in global predictions of future tropospheric ozone and aerosols, J. Geophys. Res., 111, D12304, doi:10.1029/2005JD006852, 2006.

ACPD
13, 20011–20048, 2013

McLinden, C. A., Olsen, S. C., Hannegan, B., Wild, O., and Prather, M. J.: Stratospheric ozone in 3-D models: a simple chemistry and the cross-tropopause flux, J. Geophys. Res., 105, 14653–14665, 2000.

Moxim, W. J. and Levy II, H.: A model analysis of the tropical South Atlantic Ocean tropospheric ozone maximum: the interaction of transport and chemistry, J. Geophys. Res., 105, 17393–17415, 2000.

Murray, L. T., Logan, J. A., Jacob, D. J., Hudman, R. C., and Koshak, W. J.: Spatial and inter-annual variability in lightning constrained by LIS/OTD satellite data for 1998–2006: implications for tropospheric ozone and OH, J. Geophys. Res., 117, D20307, doi:10.1029/2012JD017934, 2012.

Nakicenovic, N. and Swart, R. (eds.): Special Report on Emissions Scenarios, Cambridge Univ. Press, New York, 2000.

Novelli, P. C., Masarie, K. A., Lang, P. M., Hall, B. D., Myers, R. C., and Elkins, J. W.: Reanalysis of tropospheric CO trends: effects of the 1997–1998 wildfires, J. Geophys. Res., 108, 4464, doi:10.1029/2002JD003031, 2003.

Novelli, P. C. and Masarie, K. A.: Atmospheric Carbon Monoxide Dry Air Mole Fractions from the NOAA ESRL Carbon Cycle Cooperative Global Air Sampling Network, 1988-2011, Version: 2012-09-18, Path: ftp://aftp.cmdl.noaa.gov/data/trace_gases/co/flask/surface/, last access: 28 July 2013, 2013.

Pickering, K. E., Wang, Y., Tao, W., Price, C., and Muller, J.: Vertical distributions of lightning NO_x for use in regional and global chemical transport models, J. Geophys. Res., 103, 31203–31216, 1998.

Price, C. and Rind, D.: A simple lightning parameterization for calculating global lightning distributions, J. Geophys. Res., 97, 19919–19933, 1992.

Pye, H. O. T., Liao, H., Wu, S., Mickley, L. J., Jacob, D. J., Henze, D. K., and Seinfeld, J. H.: Effect of changes in climate and emissions on future sulfate-nitrate-ammonium aerosol levels in the United States, J. Geophys. Res., 114, D01205, doi:10.1029/2008JD010701, 2009.

Rigby, M., Prinn, R. G., Fraser, P. J., Simmonds, P. G., Langenfelds, R. L., Huang, J., Cunnold, D. M., Steele, L. P., Krummel, P. B., Weiss, R. F., O'Doherty, S., Salameh, P. K., Wang, H. J., Harth, C. M., Mühle, J., Porter, L. W.: Renewed growth of atmospheric methane, Geophys. Res. Lett., 35, L22805, doi:10.1029/2008GL036037, 2008.

ACPD
13, 20011–20048, 2013

Rinsland, C. P., Meier, A., Griffith, D. W. T., and Chiou, L. S.: Ground-based measurements of tropospheric CO, C_2H_6, and HCN from Australia at 34° S latitude during 1997–1998, J. Geophys. Res., 106, 20913–20924, 2001.

Rolph, G. D.: Real-time Environmental Applications and Display sYstem (READY) Website, NOAA Air Resources Laboratory, Silver Spring, MD, available at: http://ready.arl.noaa.gov, last access: 28 July 2013.

Schneising, O., Buchwitz, M., Reuter, M., Heymann, J., Bovensmann, H., and Burrows, J. P.: Long-term analysis of carbon dioxide and methane column-averaged mole fractions retrieved from SCIAMACHY, Atmos. Chem. Phys., 11, 2863–2880, doi:10.5194/acp-11-2863-2011, 2011.

Singh, H. B., Herlth, R., Kolyer, R., Chatfield, W., Viezee, L. J., Salas, Y., Chen, J. D., Bradshaw, S. T., Sandholm, R., Talbot, G. L., Gregory, B., Anderson, G. W., Sachse, E., Browell, A. S., Bachmeier, D. R., Blake, B., Heikes, D., Jacob, H. E., and Fuelberg: Impact of biomass burning emissions on the composition of the South Atlantic troposphere: reactive nitrogen and ozone, J. Geophys. Res., 101, 24203–24219, 1996.

Sinha, P., Jaeglé, L., Hobbs, P. V., and Liang, Q.: Transport of biomass burning emissions from Southern Africa, J. Geophys. Res., 109, D20204, doi:10.1029/2004JD005044, 2004.

Spivakovsky, C. M., Logan, J. A., Montzka, S. A., Balkanski, Y. J., Foreman-Fowler, M., Jones, D. B. A., Horowitz, L. W., Fusco, A. C., Brenninkmeijer, C. A. M., Prather, M. J.,Wofsy, S. C., and McElroy, M. B.: Three-dimensional climatological distribution of tropospheric OH: update and evaluation, J. Geophys. Res., 105, 8931–8980, 2000.

Spracklen, D. V., Mickley, L. J., Logan, J. A., Hudman, R. C., Yevich, R., Flannigan, M. D., and Westerling, A. L.: Impacts of climate change from 2000 to 2050 on wildfire activity and carbonaceous aerosol concentrations in the Western United States, J. Geophys. Res., 114, D20301, doi:10.1029/2008JD010966, 2009.

Sudo, K., Takahashi, M., Kurokawa, J., and Akimoto, H.: CHASER: a global chemical model of the troposphere, 1. Model description, J. Geophys. Res., 107, 4339, doi:10.1029/2001JD001113, 2002.

Swap, R. M., Garstang, M., Macko, S. A., Tyson, P. D., Maenhaut, W., Artaxo, P., Kållberg, P., and Talbot, R.: The long-range transport of Southern African aerosols to the tropical South Atlantic, J. Geophys. Res., 101, 23777–23791, 1996.

ACPD
13, 20011–20048, 2013

Thompson, A. M., Huntley, M. A., and Stewart, R. W.: Perturbations to tropospheric oxidants, 1985–2035 1. Calculations of ozone and OH in chemically coherent regions, J. Geophys. Res., 95, 9829–9844, 1990.

Thompson, A. M., Doddridge, B. G., Witte, J. C., Hudson, R. D., Luke, W. T., Johnson, J. E., Johnson, B. J., Oltmans, S. J., and Weller, R.: A tropical Atlantic paradox: shipboard and satellite views of a tropospheric ozone maximum and wave-one in January–February 1999, Geophys. Res. Lett., 27, 3317–3320, 2000.

Thompson, A. M., Doddridge, B. G., Witte, J. C., Hudson, R. D., Luke, W. T., Johnson, J. E., Johnson, B. J., Oltmans, S. J., and Weller, R.: Tropical tropospheric ozone and biomass burning, Science, 291, 2128–2132, 2001.

Unger, N., Shindell, D. T., Koch, D. M., Amann, M., Cofala, J., and Streets, D. G.: Influences of man-made emissions and climate changes on tropospheric ozone, methane, and sulfate at 2030 from a broad range of possible futures, J. Geophys. Res., 111, D12313, doi:10.1029/2005JD006518, 2006.

van der Werf, G. R., Randerson, J. T., Giglio, L., Collatz, G. J., Kasibhatla, P. S., and Arellano Jr., A. F.: Interannual variability in global biomass burning emissions from 1997 to 2004, Atmos. Chem. Phys., 6, 3423–3441, doi:10.5194/acp-6-3423-2006, 2006.

Wang, Y. and Jacob, D. G.: Anthropogenic forcing on tropospheric ozone and OH since preindustrial times, J. Geophys. Res., 103, 31123–31135, 1998.

Westerling, A., Hidalgo, H., Cayan, D., and Swetnam, T.: Warming and earlier spring increases Western US forest wildfire activity, Science, 313, 940–943, 2006.

Wild, O. and Palmer, P. I.: How sensitive is tropospheric oxidation to anthropogenic emissions?, Geophys. Res. Lett., 35, L22802, doi:10.1029/2008GL035718, 2008.

Wu, L., Su, H., and Jiang, J. H.: Regional simulations of deep convection and biomass burning over South America: 1. Model evaluations using multiple satellite data sets, J. Geophys. Res., 116, D17208, doi:10.1029/2011JD016105, 2011.

Wu, S., Mickley, L. J., Jacob, D. J., Logan, J. A., Yantosca, R. M., and Rind, D.: Why are there large differences between models in global budgets of tropospheric ozone?, J. Geophys. Res., 112, D05302, doi:10.1029/2006JD007801, 2007.

Wu, S., Mickley, L. J., Jacob, D. J., Rind, D., and Streets, D.: Effects of 2000–2050 changes in climate and emissions on global tropospheric ozone and the policy-relevant background ozone in the United States, J. Geophys. Res., 113, D18312, doi:10.1029/2007JD009639, 2008a.

ACPD
13, 20011–20048, 2013

Wu, S., Mickley, L. J., Leibensperger, E. M., Jacob, D. J., Rind, D., and Streets, D. G.: Effects of 2000–2050 global change on ozone air quality in the United States, J. Geophys. Res., 113, D06302, doi:10.1029/2007JD008917, 2008b.

Yevich, R. and Logan, J. A.: An assessment of biofuel use and burning of agricultural waste in the developing world, Global Biogeochem. Cy., 17, 1095, doi:10.1029/2002GB001952, 2003.

Yu, H., Chin, M., Remer, L. A., Kleidman, R. G., Bellouin, N., Bian, H., and Diehl, T.: Variability of marine aerosol fine-mode fraction and estimates of anthropogenic aerosol component over cloud-free oceans from the Moderate Resolution Imaging Spectro-radiometer (MODIS), J. Geophys. Res., 114, D10206, doi:10.1029/2008JD010648, 2009.

Zhao, T. X.-P., Laszlo, I., Guo, W., Heidinger, A., Cao, C., Jelenak, A., Tarpley, D., and Sullivan, J.: Study of long-term trend in aerosol optical thickness observed from operational AVHRR satellite instrument, J. Geophys. Res., 113, D07201, doi:10.1029/2007JD009061, 2008.

ACPD
13, 20011–20048, 2013

Table 1. Comparison of present-day and future emissions in Africa and Latin America.

Species	Northern Africa[1] (in Jan)			Southern Africa[2] (in Sep)			Latin America[3] (in Sep)		
	Present-day	future	Change (%)	Present-day	future	Change (%)	Present-day	future	Change (%)
CO (Tg)									
Biomass burning	23.4	31.1	33	22.0	13.7	−38	18.4	57.3	212
Fossil fuel	0.35	2.00	477	0.44	1.75	302	0.85	0.89	5
NO_x (Tg N)									
Biomass burning	0.18	0.20	12	0.44	0.24	−46	0.35	0.82	134
Lightning	0.042	0.034	−19	0.021	0.026	22	0.056	0.067	19
Soil	0.070	0.064	−9	0.061	0.066	8	0.093	0.097	4
Fossil fuel	0.009	0.095	956	0.039	0.189	381	0.065	0.175	171

Area defined within: [1] 0°–15° N, 15° W–35° E; [2] 35° S–0°; 10° E–40° E; [3] 40° S–0°; 80° W–35° W.

ACPD
13, 20011–20048, 2013

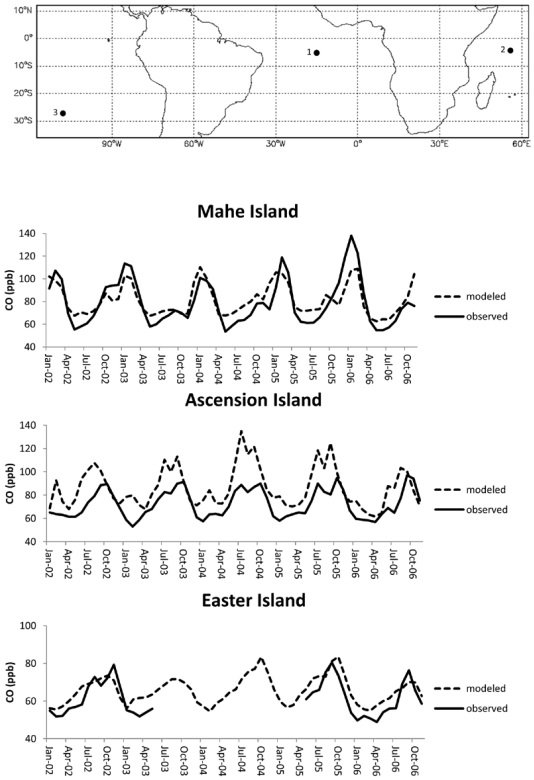

Fig. 1. Location of ground-level remote monitoring stations selected for the study (top, 1. Ascension Island, 2. Mahe Island, 3. Easter Island) and variation of CO concentrations in 2002–2006 at the three stations (bottom).

ACPD
13, 20011–20048, 2013

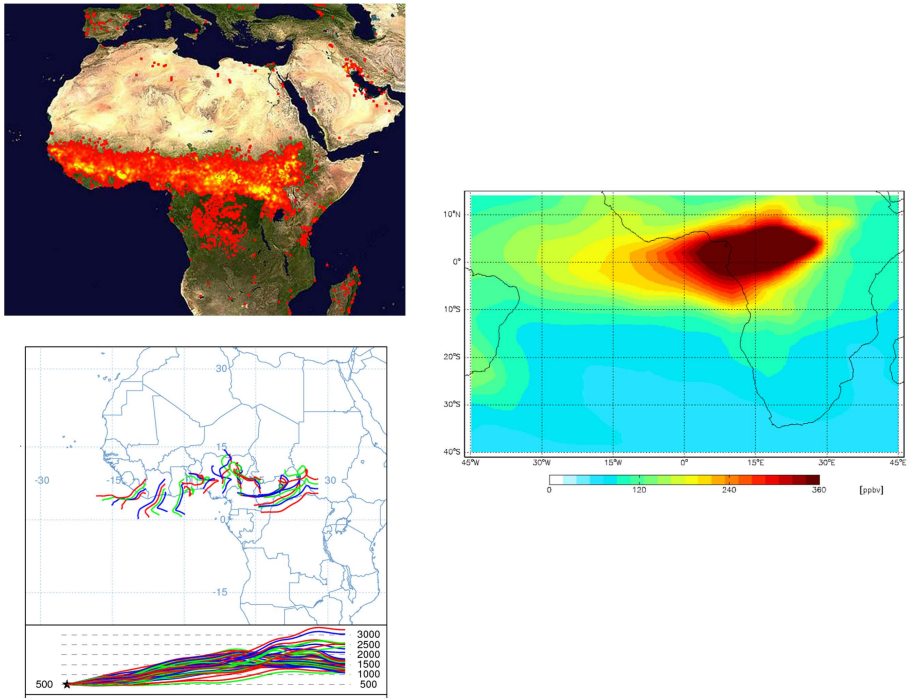

Fig. 2. A 10 day (21–30 January 2005) fire map detected by MODIS (upper left), a plot of 3.5 days forward trajectory matrix launched on 20 January 2005 from Northern Africa (lower left), and predicted monthly averaged CO concentrations (ppb) by GEOS-chem at 704 hPa in January 2005 (right).

ACPD
13, 20011–20048, 2013

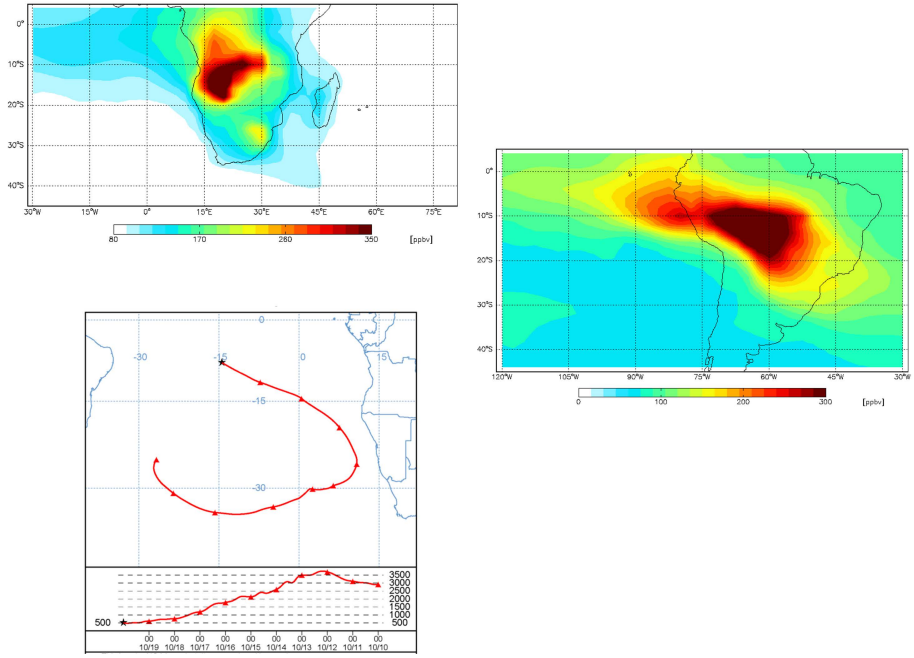

Fig. 3. Monthly averaged surface CO distribution over Southern Africa and Atlantic Ocean in September 2005 (upper left), a typical 10 day backward trajectory (launched on 20 October 2003) showing recirculation of air mass over Southern Atlantic Ocean (lower left), and monthly averaged CO concentrations (ppb) predicted by GEOS-chem model over Latin America at 704 hPa (right).

ACPD
13, 20011–20048, 2013

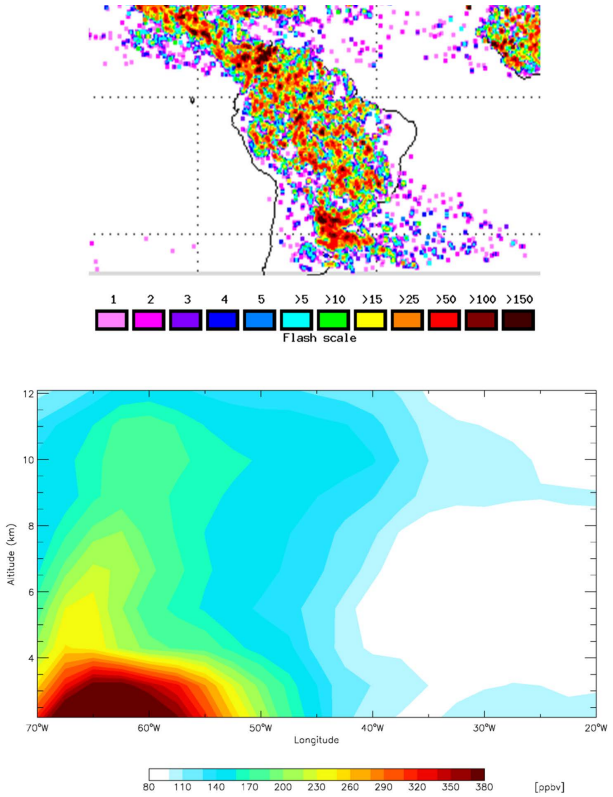

Fig. 4. Lightning events (flash/pixel/month) in September 2006 (upper) and vertical CO distribution at 14° S over burning areas of Latin America in September 2006 (lower).

ACPD
13, 20011–20048, 2013

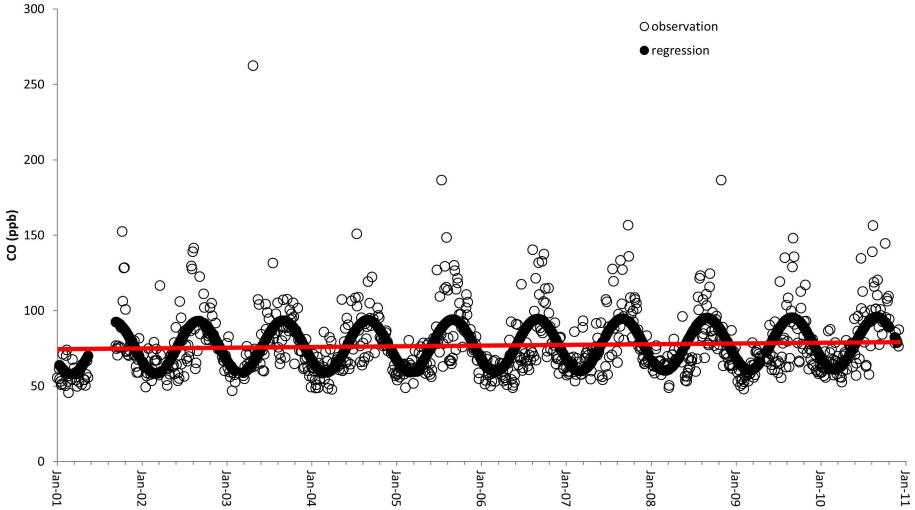

Fig. 5. Time evolution of CO concentrations (ppb) in 2001–2010 at Ascension Island. A trend line is shown in red.

ACPD
13, 20011–20048, 2013

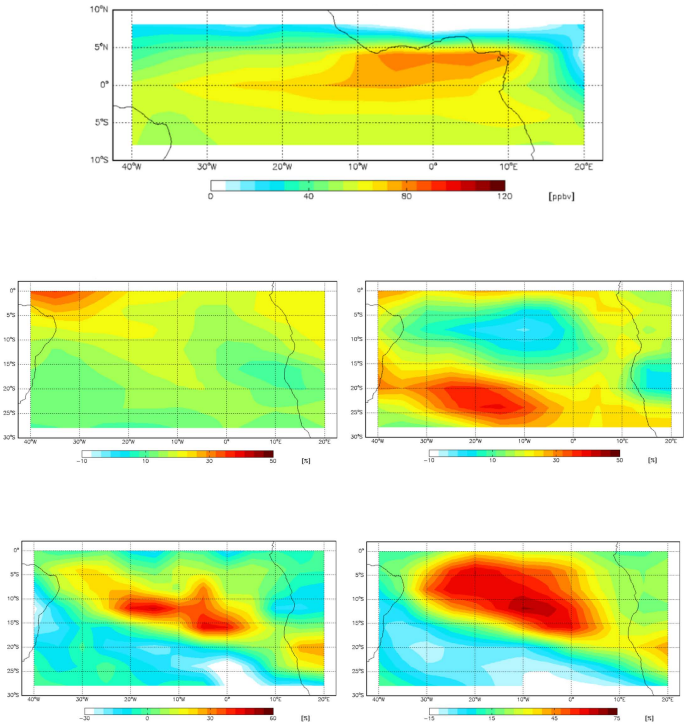

Fig. 6. Difference plot (2050s–2000s) of lower tropospheric CO distribution (ppb) over Northern Africa coast and Atlantic Ocean in January (top). The panels below show the percentage difference (2050s–2000s) of O_3 distribution in upper (middle left) and mid-troposphere (middle right); column cloud fraction (bottom left) and specific humidity in mid-troposphere (bottom right) over the SAO in January.

ACPD
13, 20011–20048, 2013

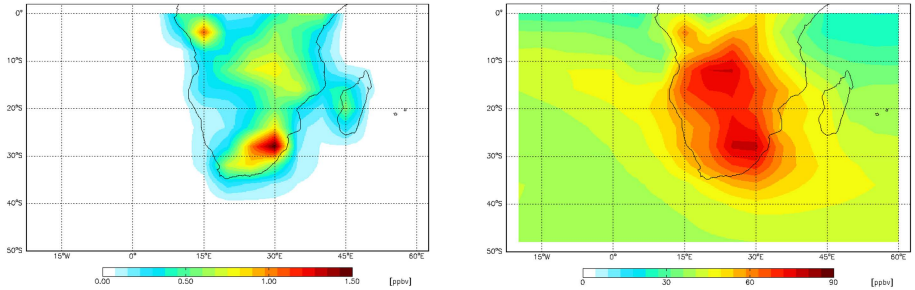

Fig. 7. Lower tropospheric NO_x (left) and O_3 (right) distribution (ppb) over Southern Africa and nearby oceanic areas in future September.

ACPD
13, 20011–20048, 2013

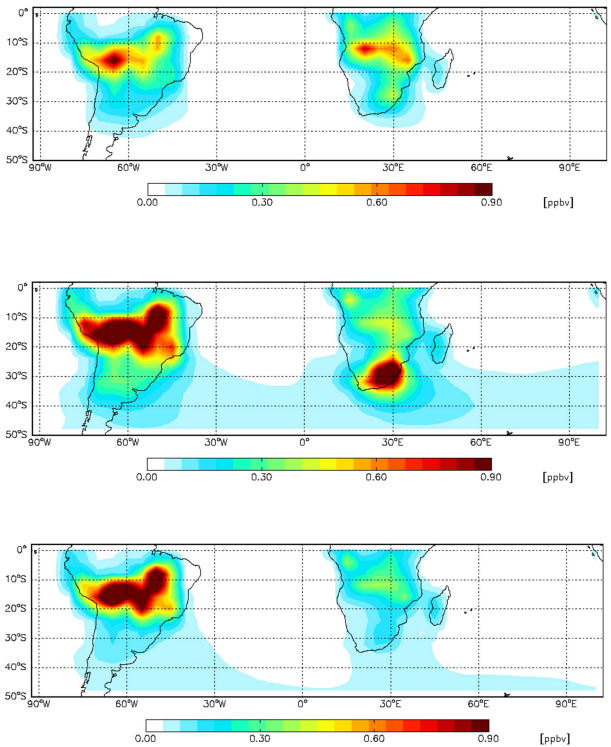

Fig. 8. Lower tropospheric PAN distribution (ppb) over Southern Africa, Latin America, the remote SAO and Indian Ocean in present September (top), future September (middle) and that excluding the fossil fuel contribution (bottom).

ACPD
13, 20011–20048, 2013

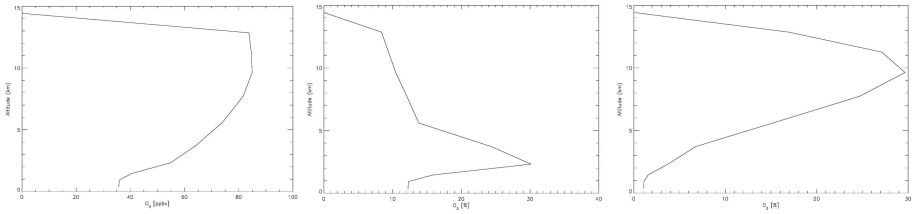

Fig. 9. Vertical profiles of total O_3 concentrations (ppb) (left) with burnings (middle) and lightning (right) contribution in percentage over the SAO (defined as an area within 25° S, 25° W and 5° S, 5° E) in future September.

ACPD
13, 20011–20048, 2013

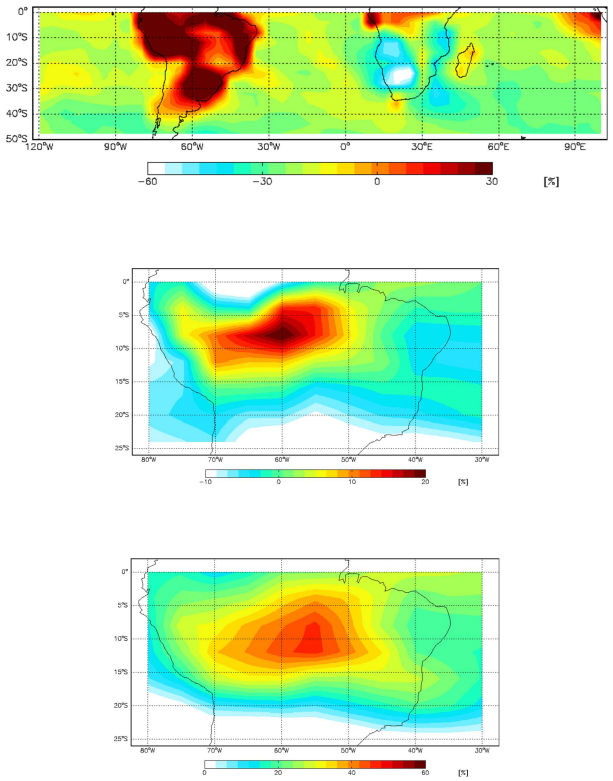

Fig. 10. Percentage difference of boundary-layer OH between present and future over tropical areas and SH in September (top). Percentage increase of OH (middle) corresponding to the increase of NO_x (bottom) in upper troposphere between present and future September over low latitudes of Latin America.

ACPD
13, 20011–20048, 2013